NEACRP-L-343
SEPTEMBER 1989

NEACRP RECOMMENDATION FOR

STANDARD DISPLACEMENT DAMAGE DOSE UNIT

Y. Orechwa
Argonne National Laboratory, U.S.A.

M. Salvatores
Commissariat à l'Energie Atomique, France

O E C D N u c l e a r E n e r g y A g e n c y

C o m m i t t e e o n R e a c t o r P h y s i c s

NEACRP RECOMMENDATION FOR

STANDARD DISPLACEMENT DAMAGE DOSE UNIT

Y. Orechwa (Argonne National Laboratory, U.S.A.)
M. Salvatores (Commissariat à l'Energie Atomique, France)

1. Introduction

There is a recognised need for an international standardisation of a displacement damage dose unit, in order to characterise material irradiations in reactors, and to compare irradiation effects in different reactors, and in different locations (i.e., different spectra) of the same reactor. Since different units (DPA according to different models, total fluence, flux above a threshold energy, etc.) have been used by different laboratories, a single agreed unit seems desirable to establish a common language to exchange data and experience.

It is currently held that the main cause of mechanical damage in materials is atomic displacements from the crystal lattice. However other effects can result from, e.g., the introduction of foreign atoms to a material by nuclear transmutation reactions, as the high temperature embrittlement related to helium production, the microstructure and purity of a material or temperature conditions during an irradiation cycle.

The uncertainty of the correlation of changes of structural material properties (i.e., swelling) to atomic displacements is then due to both the physical atom displacement model adopted and to other factors, like helium production, presence of impurities, temperature conditions effects, etc.

This last point stresses the fact that, even if the most reliable physical model of neutron-induced atomic displacement has to be sought, the inaccuracies of damage dose models are also significantly related to factors and extrapolation rules which are of a more metallurgical nature.

2. The NRT model for the definition of a unit of displacement dose

A model has been developed [1], in which the displacement cross-section of nuclide species *j*, for an incident neutron of energy *E*, is defined as :

$$\sigma_{dj}(E) = \frac{\kappa}{2E_{dj}} \sum_r \sigma_{rj}(E) \int P_{rj}(E,E')E' \frac{1}{1+K_{j,g}(E',j,j')} dE' \quad \ldots\ldots\ldots\ldots (1)$$

In this expression :

$\sigma_{rj}(E)$	: Cross-section for neutrons of energy *E* undergoing primary reaction *r* with nuclide *j*;
$P_{rj}(E,E')\,dE'$	: Probability that this reaction will produce a recoil in the energy range *E'* to *E'+dE*;
E_{dj}	: Energy required to displace an atom from the lattice of element *j* ;
κ	: Displacement efficiency accounting for departure form hard-sphere scattering;
$K_{j,g}(E',j,j')$	: Functions in the Lindhard formula for the fraction of the primary knock-on energy *E'* which is transferred elastically to the cascade.

It should be noted that the Lindhard formula makes allowance for a primary knock-on atom of one species *j'*, transferring energy to a lattice of a different species *j*, with the restriction that the atomic numbers and atomic weights must not be very different.

The NRT model strictly embraces all the factors in Equation (1) except $\sigma_{rj}(E)$ and $P_{rj}(E,E')\,dE'$. These last are in the different category of primary reaction cross-section data. From computer studies, κ has been found constant (0.8) for a range of nuclides from iron to tungsten, but the value for E_d is empirical and includes an adjustment for recombination of "near-neighbour" defects.

In practical terms, producers and users of the damage rules are concerned only with energy-dependence, so for pure elements the values of multiplicative constants κ and E_d can be imposed arbitrarily. A value E_d = 40 eV has been suggested for iron.

Given a steady-state neutron spectrum $\Phi(E)\,dE$, the number of displacements per atom in element j in a time t will be:

$$t \int \sigma_{dj}(E)\,\Phi(E)\,dE$$

3. The unit for an alloy

In the case of an alloy, a displacement model which accounts properly for the metallurgical detail in the alloy, is not available at present.

Among the users of the NRT model, two definitions have been adopted up to now :

a) Use of $\sigma_{d\,Alloy}(E) = \sigma_{dFe}$ for all alloys;

b) Use of a mixed-fraction model:

$$\sigma_{d\,Alloy}(E) = \sum_i f_i\,\sigma_{di}(E) \qquad (\sum_i f_i = 1.0) \cdots\cdots\cdots\cdots\cdots\cdots (2)$$

where f_i is the atomic fraction of species i in the alloy.

The major objection to the use of definition *(a)* is that definition fails to account for real differences among the primary reaction cross-sections in the constituent nuclides of the alloy. However, this definition is particularly simple, and has a good physical basis for the major constituent of most alloys of interest.

The major objection to definition *(b)* is that this definition assumes that a primary knock-on atom of a certain species will expend its energy in collisions with atoms of the same species, which is certainly unrealistic [2]:

To illustrate the implications of these two definitions, Table 1 gives the one-group σ_d for Fe, Cr, Ni taken separately and obtained from equation (1) and for steel, obtained from equation (2), in different spectra and reactors. Table 2 gives the energy dependence of a damage dose rate in two different positions of the same reactor.

The inspection of these tables indicates:

a) The σ_{Fe} and the $\sigma_{d\,steel}$ differ by less than 7% in the core blanket regions;

b) This difference can be larger in regions far from the core (~ ÷ 15 %), due to spectral effects.

The differences, in particular in core regions, could be comparable to the uncertainty related to a crude alloy model (the mixed-fraction model).

Finally, it is to be noticed that the σ_d value is fairly intensive to basic data effects.

4. NEACRP recommendation

In view of the arguments given in the previous paragraphs it is recommended that:

a) The NRT model should be used for separate isotopes;

b) The σ_{dFe} (NRT) should be used as a common standard displacement damage dose unit to characterise alloys irradiation. The domain of applicability of this prescription is compatible with the needs of metallurgists, since they are keen to use irradiation information on a specific alloy in as close as possible spectra, and/or to use the same unit to compare in a simple way the irradiation of different alloys in the same flux spectrum. The domain of applicability of the proposed prescription is certainly wider than prudently practical. Unacceptable errors could be encountered, if the proposed prescription is used for all alloys in completely different irradiation conditions. This would certainly represent a misuse of the proposed standard;

c) The mixed-fraction model σ_d for alloys should also be optionally supplemented. The cross-section preparation codes should allow systematically this possibility. Alloys should be treated as separate materials. In that way, if a more satisfactorily definition for alloys will be worked out and validated, it could be easily introduced in the future. This implies also, that historical irradiation characteristics should be systematically archived;

d) Efforts should be put in the development and validation of a more rigorous definition of an alloy unit. However, the solution of this problem is beyond the scope of reactor physics and concerns essentially solid state and metallurgical physics.

References

[1] M. J. NORGETT, M. T. ROBINSON, I. M. TORRENS,
"A Proposed Method of Calculating Displacement Dose Rates", Nucl. Eng. Design 33, 50 (1975).

[2] R. ANDERSON, J. ADAMSON (UKAEA), private communication.

Table 1.
One-group σ_d (NRT) for separated isotopes and for alloy

MATERIAL	SUPERPHENIX inner core	PHENIX inner core	SUPERPHENIX radial blanket	PHENIX radial blanket	SUPERPHENIX lower grid plate
Fe	250	274	121	198	24.6
Cr	287	314	137	225	30.2
Ni	305	329	168	251	49.9
Steel	263	288	129	209	28.5

Table 2.
Energy repartition (%) of the damage dose rate in different positions of the same reactor (Superphenix)

ENERGY INTERVAL	SUPERPHENIX inner core	SUPERPHENIX lower grid plate
E > 1 MeV	43.5	2.1
1 MeV > E > 0.1 MeV	46	48.1
100 keV > E > 10 keV	8.6	43
10 keV > E > 1 keV	1.9	6.3
1 keV > E > 0.1 keV	–	0.3

NEUTRONICS IN THE TOROIDAL BELT-GEOMETRY OF A SCREW PINCH REACTOR

K.A. Verschuur,
Netherlands Energy Research Foundation (ECN), Petten, The Netherlands.

Abstract

The neutronics characteristics of the Belt Screw Pinch Reactor (paper B2), which differ markedly from those for a Tokamak reactor, are studied. Transport calculations have been performed in the toroidal belt geometry using albedos and accompanying absorption data for the blanket, which are calculated with one-dimensional Sn. For this purpose the ANISN code has been modified (ANISN-ALB), and the code FURNACE developed. The results for the BSPR show a marked poloidal variation of the neutron wall loading, the heating and the tritium production. The experiences with the codes ANISN-ALB and FURNACE are promising.

1. Introduction

As part of the reactor study on the Belt Screw Pinch Reactor (BSPR) /1/ a neutronics and photonics study is performed. The neutronics and photonics of this reactor are characterized by the large volume compression of the plasma, the shift of the plasma towards the outer blanket, and the large height over width ratio of the belt-shaped toroidal vessel (fig. 1). Under these circumstances the intensity and angular distribution of the flux of primary 14 MeV neutrons impinging on the first wall is strongly dependent on the position on the wall. Hence there is a marked poloidal variation of the neutron wall loading, the tritium breeding, and the heating around the torus. These effects are studied for the BSPR, assuming a Steiner type blanket all around the torus. The calculational method used is described in section 2, and the results are given in section 3. Conclusions are drawn in the last section.

2. Calculational method used

Neutron and photon transport calculations for fusion reactors are hampered by the large dimensions of such systems as compared to the mean free path of these particles. The use of special Sn-codes as the toroidal TWOTRAN /2/ and three-dimensional Monte Carlo codes as MORSE /3/ is possible, but with a large penalty in computer time, which makes these methods not very practical for design purposes. The method presented here will give relief with respect to memory space and computer time needed.

The method is not hampered by, but on the contrary makes use of the fact that the torus dimensions are large compared to the mean free path of the neutrons in the blanket (first condition). In addition it is assumed that the torus dimensions are large compared to the thickness of the blanket (second condition) which mostly is the case in fusion reactors. The first condition makes it possible to calculate the neutron and photon transport within the torus separately by using differential albedo's for the blanket. These albedo's can be calculated once for each blanket configuration.

Due to the second condition, the nucleonics behaviour of the blanket is almost independent of the curvature of the blanket, and hence will only depend on the energy and angular distribution of the incoming neutron flux. Therefore the nucleonics of the blanket can be handled with a one-dimensional transport code.

These considerations have led to the following calculational procedure:

a. For every discrete energy and angle of incidence, a one-dimensional transport calculation for the blanket is performed, producing energy and angle dependent reflected fluxes (the albedo-data), and flux- and reaction rate distributions within the blanket (the absorption data) per unit of incoming flux. These data then constitute a data library for the blanket which is independent of reactor geometry.

b. The uncollided 14 MeV neutron flux on the first wall is calculated using a ray tracing scheme as described in ref. /4/.

c. Then the scattered flux within the torus is calculated by a multiple reflection scheme using the albedo data. This calculation gives the energy and angle dependent neutron fluxes impinging on the first wall for a series of discrete positions around the torus.

d. These incoming flux distributions are then used to weight the absorption data from the library, resulting in the flux- and reaction rate distributions in the blanket for all discrete points around the torus.
Finally these reaction rates are integrated over the blanket zones to attain the tritium breeding, thermal power production and other reaction data of the whole blanket.

The albedo data on the library are given in Sn-discretization (n=8). The multiple reflection calculation is performed with an angular quadrature which differs slightly from the Sn quadrature, in that for each level the azimuthal angles are equidistant. (For level j the x-axis is a $4(n/2-j+1)$ rotation axis).
Due to the small plasma volume in the BSPR only a few directions of the n=8 quadrature will see the plasma. Therefore the uncollided flux is calculated in a finer angular mesh, attained by subdividing each direction in m^2 directions ($m \approx 20$).

The code system consists of the code ANISN-ALB /6/ which is a modified version of the ANISN code /5/ that produces the albedo library and the absorption library, and the code FURNACE /6/, designed to perform the multiple reflection calculations in the toroidal belt geometry. It is intended to produce a second version of FURNACE which can handle more general toroidal geometries. A flow diagram of FURNACE is given in fig. 2.

3. Calculations

The torus of the BSPR has a major radius of 10 m, a width of 5 m and a height of 15 m (fig. 1). It is surrounded by a "Steiner" blanket consisting of a first wall of 1 cm SS, a lithium zone of 60 cm and a reflector zone of 15 cm iron. The lithium zone contains 90% natural Li, 5% SS and 5% void for the cooling. The plasma geometry resulting from plasma equilibrium /8/ is also shown in fig. 1. The volume compression of the plasma $\kappa_V = 20.3$ and the outward shift of the plasma $\Delta/b = 0.28$. Calculations are performed for a fusion power of 5 GW produced homogeneously in the plasma.
Cross sections and kerma factors have been taken from the EPR-library /7/. A macroscopic cross section library was produced, which then was condensed to 7 neutron groups and 3 gamma groups by a ANISN condensation run for the blanket. Then a 10 group albedo library and absorption library was produced with the ANISN-ALB code.
Finally the FURNACE code was run for the BSPR-reactor. For the 10 energy groups the ANISN-ALB run took 250 cp seconds and the FURNACE run took 135 cp seconds on a CYBER-175. Computer time will increase quadratically with the number of energy groups for ANISN-ALB, and linearly for

FURNACE. Calculations in more energy groups will be performed in the near future /6/.

Prior to the full calculation for the BSPR, the influence of the aspect ratio A and the height over width ratio e of the belt shaped torus, on the wall load distribution was studied, taking into account the influence of A and e on the plasma geometry /8/. The calculations revealed that within the range of $2 \leq A \leq 5$ and $2 \leq e \leq 3$, the ratio of the maximum to average wall loading lies within 10% of the average value.

Poloidal distributions of the neutron wall loading P_w and the thermal power produced per m^2 wall surface P are given in figure 3. Poloidal distributions of the tritium production per m^2 wall surface (T, T_6, T_7) are given in figure 4. It can be seen that the variation of the neutron wall loading is pronounced. The variation of T7 is even more pronounced, owing to the slant incidence of the 14 MeV neutrons on the upper and lower parts of the inner and outer walls. Due to this the loss of neutrons below the threshold of the ^7Li reaction by inelastic scattering in the first wall is increased. Neutron flux profiles, which are not given here, show that especially at higher energies there is a nett flow of neutrons out of the high flux regions (the mid regions of the inner and outer blanket) into the torus, and a nett flow of neutrons from the torus into the low flux regions (the upper and lower parts of the inner and outer blanket). This explains the less pronounced poloidal variation of the tritium production by the ^6Li reaction T6, and of the thermal power production P. The fast neutron flux, the epithermal flux and the thermal flux in the first wall, which are a measure for the neutron radiation damage and the activation of the first wall, are also given in fig. 3.

The radial distributions of the heating rates p and the tritium production rates t in the blanket are given in figures 5 and 6 for a few positions around the torus (positions are indicated in fig. 1). The influence of the slant incidence of the 14 MeV neutrons on the distribution of t7 and p in the low flux regions can be seen very clearly. The increased slope of t6 in the low flux regions is also due to the slant incidence, in that it reduces the effective slowing down length of the neutrons. The integral data for the inner, upper + lower and outer blanket, as given in the table, reflect the above mentioned effects.

The neutron energy multiplication Q_n and the breeding ratio T for the whole blanket are rather low due to the absence of a lithium layer behind the iron reflector.

4. Conclusions

These first calculations show that the method proposed here can give good insight in the neutronics and photonics in a toroidal fusion reactor at low computing costs. It is believed that even if more energy groups are used to attain greater accuracy, computing time will still be lower than for example if a two-dimensional transport code is used. This will be even more the case, if the albedo- and absorption libraries are used for a series of FURNACE calculations.

The large ratios of maximum to average wall loading and of maximum to average power production in the blanket, will have consequences with respect to the technical design of the BSPR /1/. If the inner blanket is replaced by a neutron reflector, as suggested in /1/, more attention will have to be paid to the optimalisation of the tritium breeding ratio.

The high energy multiplication of the blanket desired for the BSPR might become a problem. Further study on these subjects and more experiences with the method will be given in /6/.

References

/1/ Bustraan, M. et al., "A Reactor Study on a Belt-Shaped Screw Pinch", this conference, paper B2.

/2/ Abdou, M.A. and Jung, J., "Nuclear Analysis of a Tokamak Experimental Power Reactor Conceptual Design", Nuclear Technology, vol. 35, Aug. 1977.

/3/ Casali, F.F. et al., "FINTOR1, A Minimum Size Tokamak DT Experimental Reactor", JRC Euratom-Ispra.

/4/ Price, W.G. and Chapin, D.L., "Neutron Wall Load Distributions in a Circular Cross Section Tokamak", MATT-1102.

/5/ Devillers, C., "Systeme ANISN", CEA-N-1358.

/6/ Verschuur, K.A., "Neutronics in the Toroidal Belt-Geometry of a Screw-Pinch Reactor", ECN-report to be published.

/7/ Ford, W.E. et al., "Modification Number One of the Coupled 100 n - 21 γ Cross Section Library for EPR Calculations", ORNL/TM-5249.

/8/ Hoekzema, J.A., FOM-Rijnhuizen, Jutphaas, private communication.

Table I. Neutronics results for the BSPR.

		inner blanket	upper + lower blanket	outer blanket	total blanket
neutron wall load $\overline{P}_w$ (MW/m^2)		1.29	1.18	2.10	1.60
thermal power P_{th} (GW)		1.03	0.97	2.41	4.41
energy mult. (neutr.) Q_n		1.13	1.30	0.97	1.07
tritium breeding ratios	TR7*	0.471	0.577	0.459	
	TR6	0.799	0.883	0.594	
	T7*	0.104	0.104	0.275	0.482
	T6	0.176	0.159	0.356	0.691
	T	0.280	0.263	0.631	1.17

* T is tritium breeding per fusion.
TR is tritium breeding per incoming fusion neutron.

Fig. 1 Belt-shaped torus of the BSPR with plasma and blanket

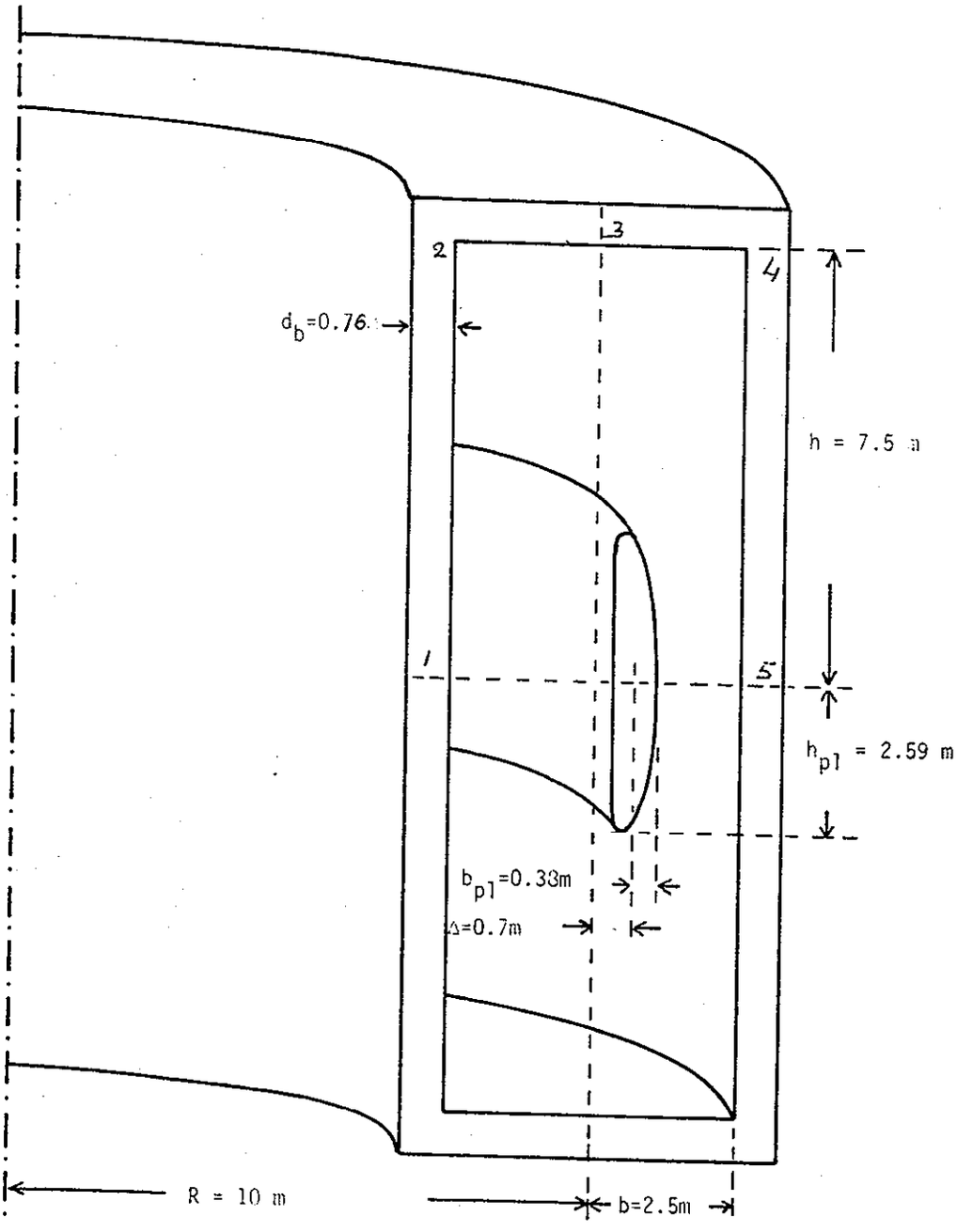

Fig. 2 Flow Diagram of FURNACE

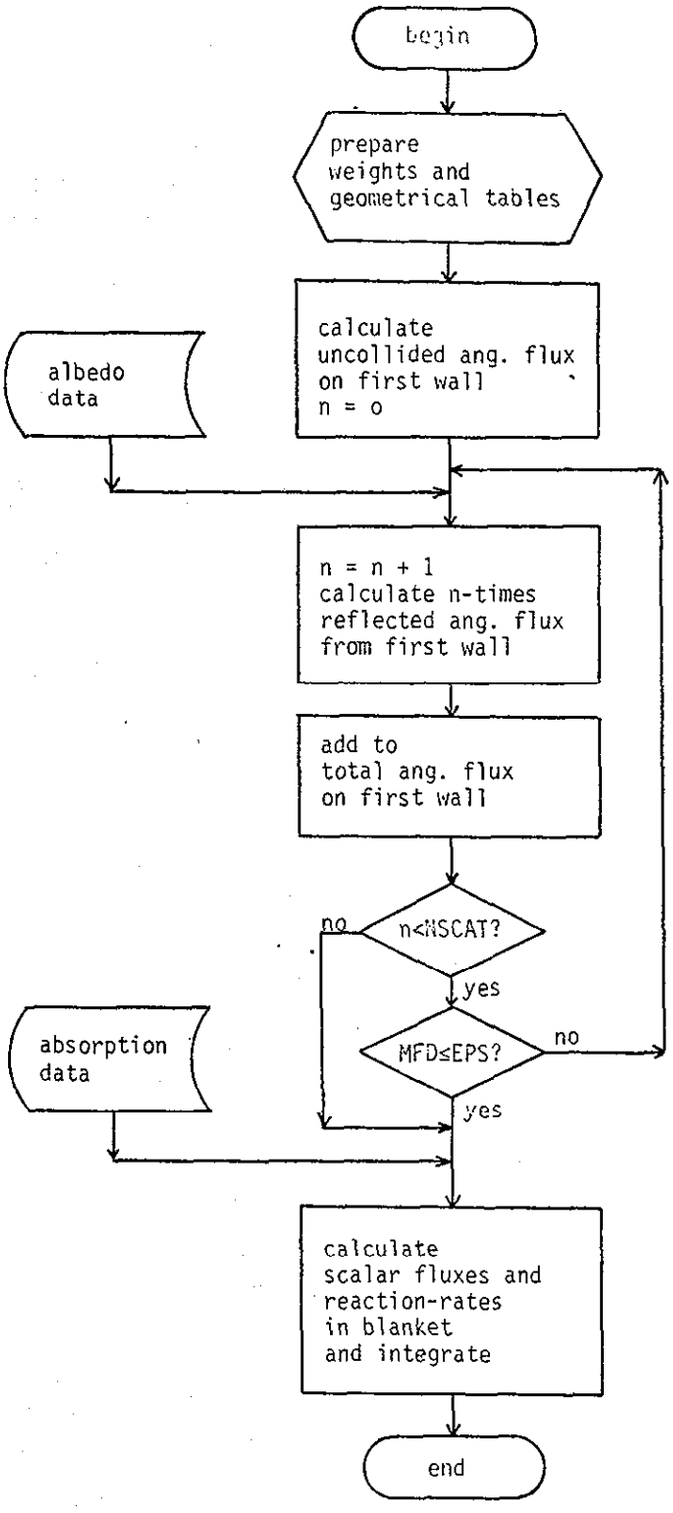

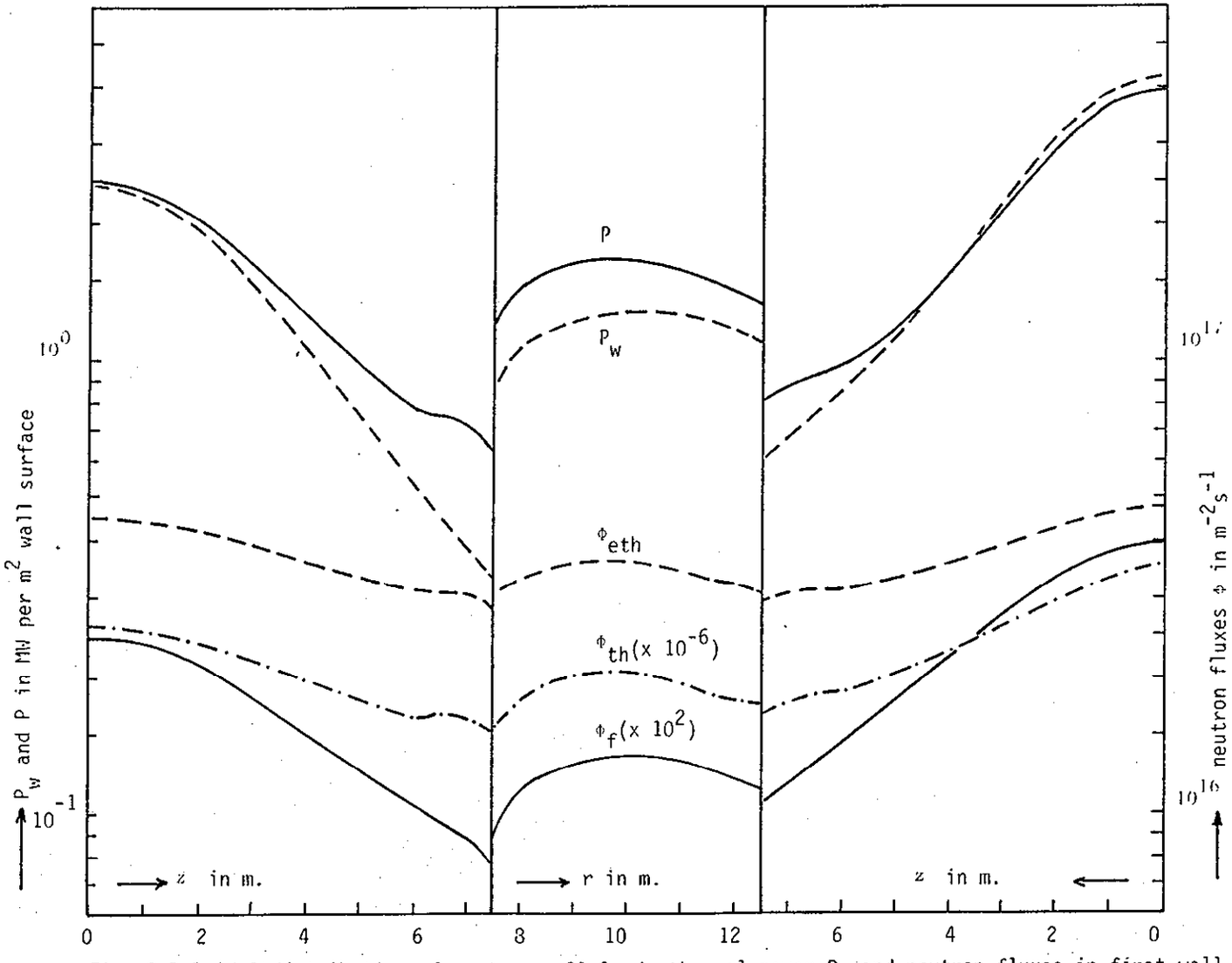

Fig. 3 Poloidal distribution of neutron wall load, thermal power P, and neutron fluxes in first wall Φ

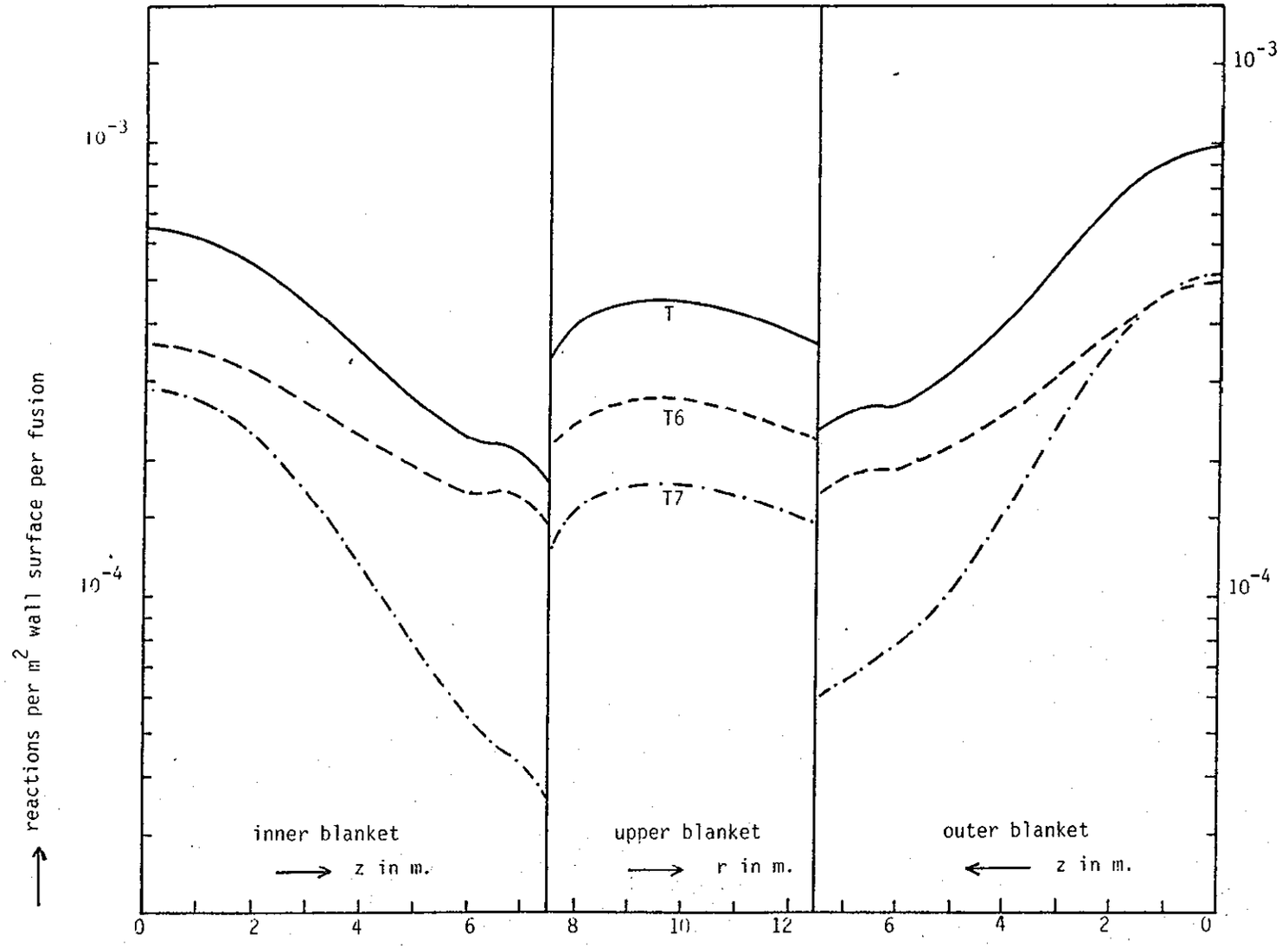

Fig. 4 Poloidal distribution of tritium breeding T

Fig. 5 Radial distribution of power density p

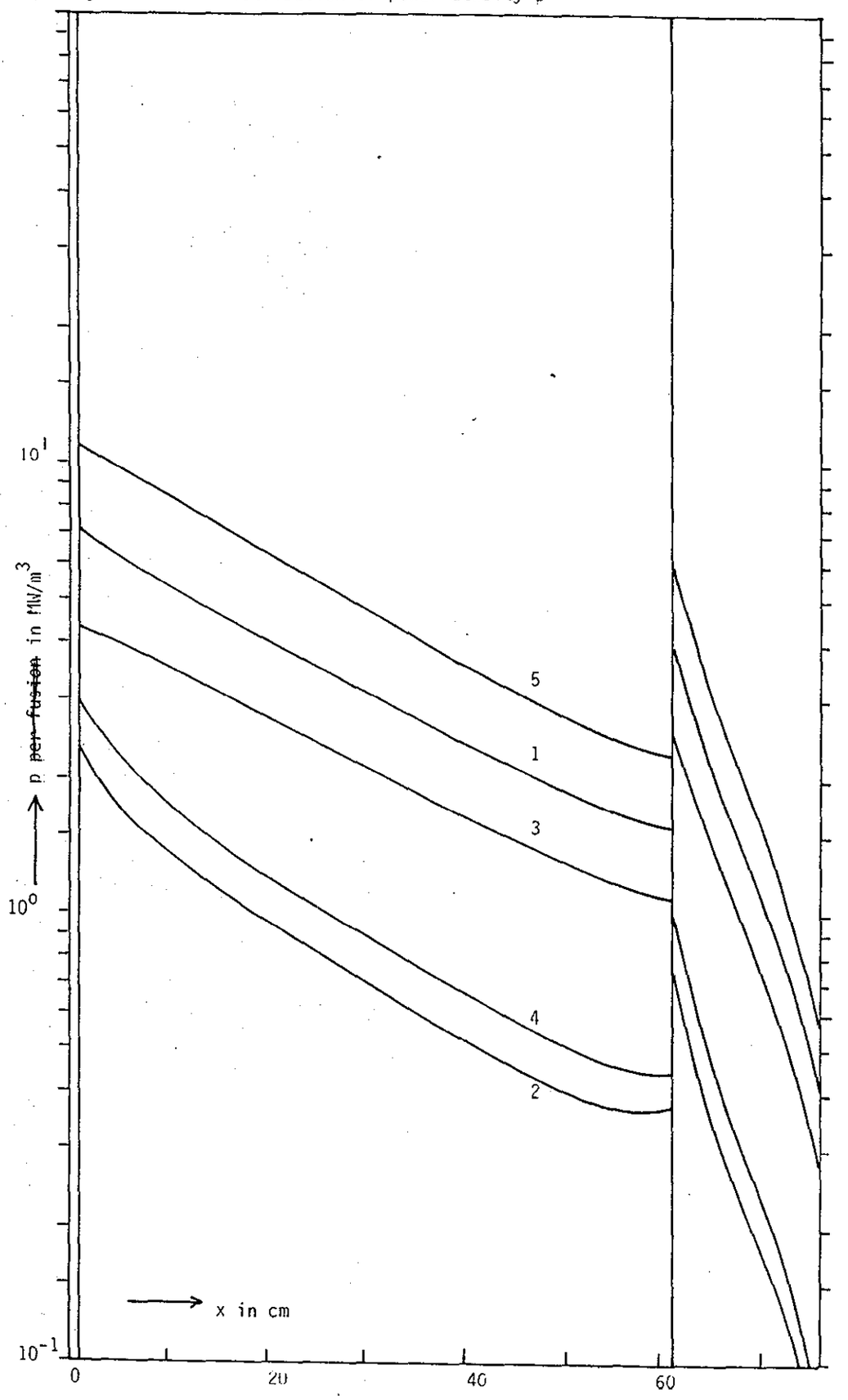

Fig. 6 Radial distribution of tritium production t per m^3